

# “Swimming” versus “swinging” effects in spacetime

Eduardo Guéron\*

*Departamento de Matemática Aplicada, Instituto de Matemática, Estatística e Computação Científica  
Universidade de Campinas, 13083-970, Campinas, SP, Brazil*

Clóvis A. S. Maia<sup>†</sup> and George E. A. Matsas<sup>‡</sup>

*Instituto de Física Teórica, Universidade Estadual Paulista, 01405-900, São Paulo, SP, Brazil*

Wisdom has recently unveiled a new *relativistic* effect, called “spacetime swimming”, where quasi-rigid free bodies in curved spacetimes can “speed up”, “slow down” or “deviate” their falls by performing “*local*” cyclic shape deformations. We show here that for fast enough cycles this effect dominates over a *non-relativistic* related one, named here “space swinging”, where the fall is altered through “*nonlocal*” cyclic deformations in Newtonian gravitational fields. We expect, therefore, to clarify the distinction between both effects leaving no room to controversy. Moreover, the leading contribution to the swimming effect predicted by Wisdom is enriched with a higher order term and the whole result is generalized to be applicable in cases where the tripod is in large red-shift regions.

PACS numbers: 01.55.+b, 04.20.-q, 45.10.Na

Recently, Wisdom unveiled a new beautiful *relativistic effect* [1] (see also Ref. [2]) denominated *spacetime swimming*, where quasi-rigid free bodies in curved spacetimes can “speed up”, “slow down” or “deviate” their falls by performing “*local*” cyclic shape deformations (see Fig. 1). This is a full general-relativistic geometrical phase effect [3], which vanishes in the limit where the gravitational constant  $G \rightarrow 0$  or the light velocity  $c \rightarrow \infty$ . Similarly to the displacement attained by swimmers in low Reynolds number fluids [4]-[5], the displacement attained by swimmers in some given spacetime only depends on their local stroke.

The fact that the swimming effect is purely relativistic has caused some perplexity [6]-[7], since it has been known for a long time that there is a similar *classical effect* in non-uniform Newtonian gravitational fields, which is present when  $c \rightarrow \infty$ . For example, an orbiting dumbbell-shaped body can modify its trajectory by contracting the strut connecting the two masses at one point and expanding it at another one [8]. We stress here that this is a *nonlocal* effect, which appears due to the fact that the work performed by the dumbbell engine against the gravitational tidal force during the contraction differs from the one during the expansion. It is the resulting net work what allows the dumbbell to change from, say, a bounded to an unbounded orbit (see Fig. 2). The shorter is the period of the whole contraction-expansion process, the smaller is the change of the trajectory, although this cannot be made arbitrarily small if one requires that the deformation velocity does not exceed  $c$ . This is in analogy with playground swings, where the oscillation amplitude is modified by an individual through standing and squatting in synchrony with the swing motion [9].

Here we perform a direct numerical simulation for a falling tripod to show that for fast enough cyclic deformations the swimming effect dominates over the swinging effect, while for slow enough cycles the opposite is true.

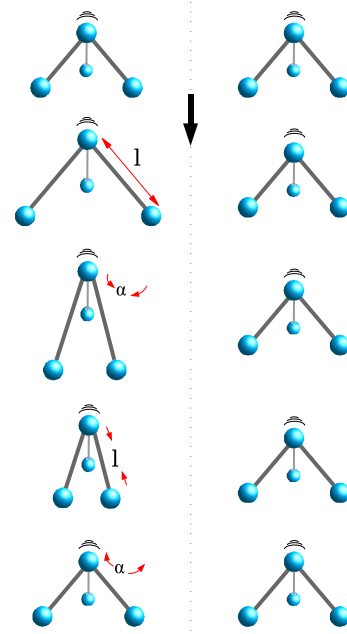


FIG. 1: Five snapshots of two tripods designed to have legs with length  $l$  and angle  $\alpha$  with the radial axis, along which they fall down, are shown with and without cyclic deformations, respectively. The swimming effect consists in realizing that *local* cyclic deformations lead, in general, to displacements of order  $G/c^2$  in the quasi-rigid tripod trajectory when compared with the rigid one.

We expect, thus, to set down any confusion concerning the dependency of both effect. In addition, we calculate and discuss the idiosyncratic features of a higher order term beyond the leading one obtained by Wisdom and extend the whole result to be applicable in cases where the tripod is in large red-shift regions.

Let us begin considering a tripod falling along the radial axis in the Newtonian gravitational field of a spher-

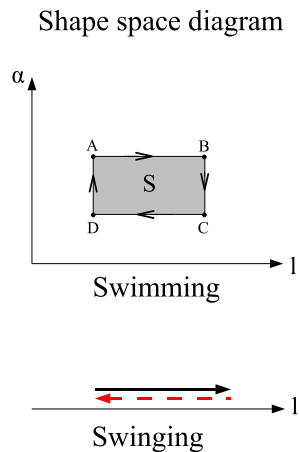


FIG. 2: The top figure carries the information that the swimming effect is a result of the non-zero area of the square (in the shape space diagram) associated with the body deformation. Were the deformation such that the area were null, the swimming effect would vanish. The bottom figure illustrates precisely this situation. Space displacements can be achieved in this case, however, through the swinging effect, i.e. by expanding and contracting the legs at *different* points of the trajectory.

ically symmetric static body with mass  $M$ . The three tripod endpoint masses  $m_i$  ( $i = 1, 2, 3$ ) are connected to the mass  $m_0$  at the vertex through *straight massless* struts with length  $l$ . The tripod is set with its vertex mass above the three endpoint masses and aligned symmetrically with the radial axis in order that the three struts make a common angle  $\alpha$  with it (see Fig. 3). The tripod legs are designed to *contract and expand*,  $l = l(t)$ , and *open and close*,  $\alpha = \alpha(t)$ , as much as  $\Delta l$  and  $\Delta \alpha$ , respectively, along a complete cycle as ruled *a priori* by some internal engine. The Lagrangian used in the action  $S = \int L dt$  to describe the falling tripod is

$$L = \sum_{a=0}^3 \frac{GMm_a}{r_a} + \sum_{a=0}^3 \frac{m_a}{2} \left( \dot{r}_a^2 + r_a^2 \dot{\theta}_a^2 + r_a^2 \sin^2 \theta_a \dot{\phi}_a^2 \right) \quad (1)$$

where “ $\dot{\phantom{x}}$ ”  $\equiv d/dt$ . The positions of the masses  $m_a$ ,  $a = 0, 1, 2, 3$ , are given through usual spherical coordinates  $r_a, \theta_a, \phi_a$  with origin at the central mass  $M$ . The tripod is not assumed to rotate,  $\dot{\phi}_i = 0$ , and the underlying symmetry guaranties that  $r_i = r_j$  and  $\theta_i = \theta_j$  for  $i, j = 1, 2, 3$ . The evolution  $r_0 = r_0(t)$  ( $\theta_0 = \phi_0 = 0$ ) of  $m_0$  is given by numerically integrating the corresponding Euler-Lagrange equations with the constraints

$$r_i = (r_0^2 + l^2 - 2r_0l \cos \alpha)^{1/2}, \quad \theta_i = \arcsin((l/r_i) \sin \alpha) \quad (2)$$

and  $\phi_i = 2\pi(i-1)/3$ . Here we consider  $r_0$  and  $p_{r_0}$  as the only independent dynamical variables. ( $r_i$  and  $\theta_i$  are implicit functions of  $r_0$  through Eq. (2).) The solid line

in Fig. 4 shows how much a quasi-rigid tripod changing shape as shown in Fig. 1 fails to follow a rigid one at the end of a complete cycle, where both tripods are let free simultaneously and we have assumed that each quarter of the whole cycle takes as long as  $T/4$  of the total period  $T$ . (For the sake of comparison we use the position of  $m_0$ .) Clearly the slower (faster) is the cycle, the larger (smaller) is  $\Delta^C r_0$ .

Let us examine in detail the high-frequency shape deformation region,  $\omega \equiv 1/T \gg \sqrt{GM/(r_0^2 \Delta l)}$ , for the sake of further comparison with the swimming effect. By “high-frequency” we mean that along the whole period  $T$  the tripods do not fall much in comparison with  $\Delta l$ . We shall assume in this regime that  $p_{r_0}$  is arbitrarily small and approximately conserved:  $p_{r_0} = \partial L / \partial \dot{r}_0 \approx 0$ . As a result one obtains, for  $m_i = m_j$ ,  $i, j = 1, 2, 3$ ,

$$dr_0 \approx U dl + V d\alpha, \quad (3)$$

where  $dr_0 = \dot{r}_0 dt$  and

$$U = - \frac{(\partial r_1 / \partial r_0) (\partial r_1 / \partial l) + r_1^2 (\partial \theta_1 / \partial r_0) (\partial \theta_1 / \partial l)}{m_0 / (3m_1) + (\partial r_1 / \partial r_0)^2 + r_1^2 (\partial \theta_1 / \partial r_0)^2}$$

and

$$V = - \frac{(\partial r_1 / \partial r_0) (\partial r_1 / \partial \alpha) + r_1^2 (\partial \theta_1 / \partial r_0) (\partial \theta_1 / \partial \alpha)}{m_0 / (3m_1) + (\partial r_1 / \partial r_0)^2 + r_1^2 (\partial \theta_1 / \partial r_0)^2}.$$

The net translation accomplished after the complete cycle ABCDA shown in Fig. 2, which circumvents an area  $S$ , can be computed using the Stokes theorem

$$\Delta^C r_0 \approx \int_{\partial S} (\partial V / \partial l - \partial U / \partial \alpha) dl \wedge d\alpha, \quad (4)$$

where  $dl$  and  $d\alpha$  are treated as one-forms in the shape space manifold covered with coordinates  $\{l, \alpha\}$ . Now, because  $\partial U / \partial \alpha = \partial V / \partial l$  [see Eq. (2)], we have that in this regime  $\Delta^C r_0 \approx 0$ . Indeed, by associating the gravitational potential energy gained by the tripod along the process with the work performed against the gravitational tidal forces, we can estimate that

$$\Delta^C r_0 \approx aGMl\Delta l / (r_0^4 \omega^2) \quad (5)$$

where  $a$  is a constant, which depends on the detailed geometry of the body. For the parameters chosen in Fig. 4  $a \approx 0.1$ . The fact that  $\Delta^C r_0 \xrightarrow{\omega \rightarrow \infty} 0$  is a general result because in the high-frequency regime the one-form  $dr_0$  will be approximately closed for any classical (or, even, semi-classical) potentials with no velocity dependence. Free-falling panicking individuals performing fast cyclic motions in Newtonian-like gravitational fields will not be able to change significantly their trajectories despite the strength of their local stroke; it had better that they swing suitably with low frequencies.

Next, let us investigate how the above picture is modified when one replaces the Newtonian gravitational field

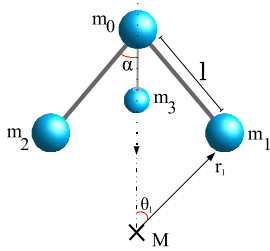


FIG. 3: The positions of the masses  $m_a$  ( $a = 0, 1, 2, 3$ ) are given through usual spherical coordinates  $r_a, \theta_a, \phi_a$  with origin at the central mass  $M$ .

by the curved Schwarzschild spacetime associated with a spherically symmetric body with mass  $M$  as described by the line element

$$ds^2 = f(r)c^2 dt^2 - f(r)^{-1} dr^2 - r^2(d\theta^2 + \sin^2 \theta d\phi^2), \quad (6)$$

where  $f(r) = 1 - 2GM/c^2 r$ . The Lagrangian used in the action  $S = \int L dt$  to evolve the tripod is

$$L = \sum_{a=0}^3 m_a \left( c^2 \dot{f}_a - \dot{r}_a^2 f_a^{-1} - r_a^2 \dot{\theta}_a^2 - r_a^2 \sin^2 \theta_a \dot{\phi}_a^2 \right)^{1/2} \quad (7)$$

where  $f_a \equiv f(r_a)$  and “ $\dot{\phantom{x}}$ ”  $\equiv d/dt$ . The constraints  $r_1 = r_1(r_0, l, \alpha)$  and  $\theta_1 = \theta_1(r_0, l, \alpha)$  are obtained in this case by requiring that the tripod struts be geodesics in the  $t \approx \text{const}$  space section of the static observers (with

4-velocity  $u \propto \partial/\partial t$ ), who measure  $l = l(t)$  as the struts’ proper length and  $\alpha = \alpha(t)$  as the proper angle of the struts with the radial axis. (The “ $\approx$ ” used above is because although we are in the high-frequency regime, it takes some time to complete each cycle.) Now, it is convenient to expand Eq. (7) up to order  $v^2/c^2$  to avoid nonlinear equations. We obtain, then, in the high-frequency regime,  $\omega \equiv 1/T \gg \sqrt{GM f_0^{1/2}/(r_0^2 \Delta l)}$  with  $T$  being the total *coordinate* period, the relativistic analogue of Eq. (3):

$$dr_0 \approx X dl + Y d\alpha, \quad (8)$$

where

$$X = \frac{-(\partial r_1/\partial r_0)(\partial r_1/\partial l) - f_1 r_1^2 (\partial \theta_1/\partial r_0)(\partial \theta_1/\partial l)}{(m_0/3m_1)(f_1/f_0)^{3/2} + (\partial r_1/\partial r_0)^2 + f_1 r_1^2 (\partial \theta_1/\partial r_0)^2}$$

and

$$Y = \frac{-(\partial r_1/\partial r_0)(\partial r_1/\partial \alpha) - f_1 r_1^2 (\partial \theta_1/\partial r_0)(\partial \theta_1/\partial \alpha)}{(m_0/3m_1)(f_1/f_0)^{3/2} + (\partial r_1/\partial r_0)^2 + f_1 r_1^2 (\partial \theta_1/\partial r_0)^2}.$$

Afterwards, we integrate Eq. (8),

$$\Delta^R r_0 \approx \int_{\partial S} (\partial Y/\partial l - \partial X/\partial \alpha) dl \wedge d\alpha, \quad (9)$$

along the complete cycle ABCDA (see Fig. 2), obtaining for small enough  $l/r_0$  and  $\Delta\alpha, \Delta l$

$$\Delta^R r_0 \approx \frac{-3m_0 m_1}{(m_0 + 3m_1)^2} \frac{GM}{c^2 r_0} \sqrt{f_0} \left[ \frac{l^2}{r_0^2} + \left( \frac{3m_1}{m_0} \sqrt{f_0} + \frac{m_0 - 3m_1}{m_0 + 3m_1} \frac{GM}{c^2 r_0 \sqrt{f_0}} \right) \frac{l^3}{r_0^3} \cos \alpha \right] \sin \alpha \Delta \alpha \Delta l \quad (10)$$

which corresponds to a proper distance  $\Delta\lambda \approx \Delta^R r_0/\sqrt{f_0}$  as measured by the static observers assuming  $\Delta^R r_0/r_0 \ll 1$ . A numerical integration of Eq. (8) with no restriction on  $\Delta\alpha$  and  $\Delta l$  was performed and is in agreement with Eq. (10) in the proper limit. Assuming that the leading term in this equation dominates over the next order one, we conclude that  $\Delta\lambda \ll \Delta l$ . The term of order  $l^2/r_0^2$  in Eq. (10) coincides with the result obtained in Ref. [1] for  $r_0 \gg 2GM/c^2$  and goes beyond, since it also holds close to the horizon:  $r_0 \gtrsim 2GM/c^2$ . It is interesting to note that the leading term of  $\Delta^R r_0$  tends to decrease as the tripod approaches the horizon. This can be understood from the fact that assuming that  $l$  is fixed, the coordinate size of the tripod decreases as  $l\sqrt{f_0}$ . As a result, the tripod is only able to probe smaller *coordinate* size regions. Now, close to the horizon the  $t - r$  section of the Schwarzschild line el-

ement (6) can be approximated ( $\theta, \phi \approx \text{const}$ ) by the Rindler wedge one [10]:  $ds^2 \approx (\rho c^2/4GM)^2 c^2 dt^2 - d\rho^2$ , where  $\rho = (4GM/c^2)/\sqrt{f(r)^{-1} - 1}$ , which has vanishing curvature. Thus, for the same reason  $\Delta^R r_0$  *vanishes* in *flat* spacetimes, this is *damped* in the *horizon’s neighborhood*. Clearly, it remains the fact that the corresponding  $\Delta\lambda$  not only is not damped but increases as the tripod approaches the horizon, as a consequence of the fact that the space curvature gets larger. Concerning the next order term, it is interesting to note that it can be positive, negative or null depending on the masses and tripod position.  $\Delta^R r_0$  is plotted in Fig. 4 (see dashed line) as a constant in the *high-frequency* region. We have taken care to keep the deformation velocity  $v < c$ . For the frequency range shown in the Fig. 4, we have  $10^{-2} \lesssim v/c \lesssim 10^{-1}$ . We see that for high enough frequencies the swimming effect can dominate the swinging effect by

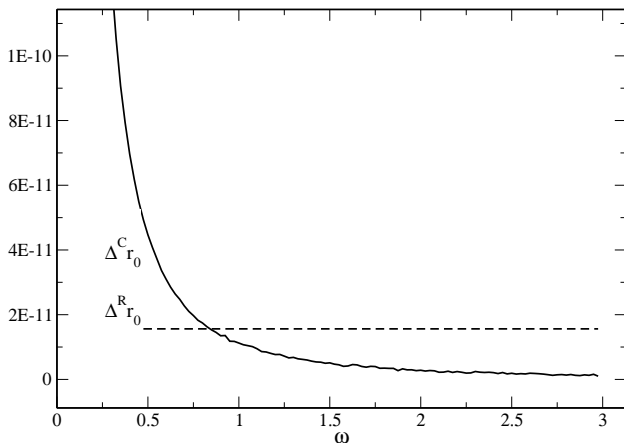


FIG. 4: The full and dashed lines show  $\Delta^C r_0 \equiv (r_0^{\text{quasi-rigid}} - r_0^{\text{rigid}})_{\text{clas}}$  and  $\Delta^R r_0 \equiv (r_0^{\text{quasi-rigid}} - r_0^{\text{rigid}})_{\text{rel}}$ , i.e. how much a free falling quasi-rigid tripod fails to follow a rigid one at the end of a complete cycle assuming a Newtonian gravitational field and a Schwarzschild spacetime characterized by a central mass  $GM = 1$ , respectively. Here the tripod is assumed to change its shape as shown in Fig. 1 and  $\omega \equiv 1/T$  is the cycle frequency. The rigid and quasi-rigid tripods are set free simultaneously with  $Gm_a = 0.1$  and  $r_0 = 100$  ( $a = 0, 1, 2, 3$ ). Initially  $\alpha = 1$  and  $l = 1$  and they vary as much as  $\Delta\alpha = -0.01$  and  $\Delta l = 0.01$  along the cycle. Each quarter of the whole cycle takes as long as  $T/4$ . (Here  $c = 1$ .)

orders of magnitude. For the parameters chosen in the graph, the swimming effect begins to dominate over the swinging effect at  $\omega \gtrsim 0.9$ . This can be estimated analytically quite well by equating Eqs. (5) and (10). A full general-relativistic numerical simulation, which would involve formidable difficulties associated with the relativistic rigid body concept, is expected to approach smoothly the swinging and swimming predictions in the low- and high-frequency regions, respectively. (For a movie on the swinging and swimming effects see Ref. [11].)

It seems to be a challenging problem to take into account the decrease of the quasi-rigid body mass (i.e. rest energy) as a consequence of the swimming. This is desirable when the work  $W$  spent (or gained) along the process is of order of  $(m_0 + 3m_1)c^2$ . The work associated with a displacement  $\Delta^R r_0$  can be estimated for  $W \ll (m_0 + 3m_1)c^2$  to be

$$W \approx (m_0 + 3m_1)GM\Delta^R r_0/(f_0 r_0^2), \quad (11)$$

where  $\Delta^R r_0/r_0 \ll f_0 r_0 c^2/(GM)$ . Eq. (11) suggests that this is very costly to swim close to the horizon. Actually, even far away from it, we do not expect the tripod to be able to climb upwards the space. This can be seen as follows. Along a complete period  $T$ , the free rigid tripod falls down about  $\Delta^F r_0 \approx GM f_0 T^2/(2r_0^2)$ . By impos-

ing that the deformation velocity  $v \lesssim c$ , we obtain  $T \gtrsim l/(c\sqrt{f_0})$  and, thus,  $\Delta^F r_0 \gtrsim GMl^2/2c^2 r_0^2 > \Delta^R r_0$ . This raises the interesting “engineering” issue concerning what would be the most efficient geometry and stroke for quasi-rigid spacetime swimming bodies. In this vein, it would be also interesting to see how the tripod could accomplish more complex maneuvers through asymmetric deformations. This is remarkable that General Relativity, which is a quite studied ninety-years-old theory did not loose its gift of surprising us. After all, free-falling panicking individuals may change their trajectories by doing fast cyclic motions because the world is relativistic.

EG is indebted to J. Wisdom for various conversations and P. Letelier for the support. Two of us, CM and GM, would like to acknowledge full and partial financial supports from Fundação de Amparo à Pesquisa do Estado de São Paulo, respectively, while GM is also thankful to Conselho Nacional de Desenvolvimento Científico e Tecnológico for partial support.

---

\* e-mail: gueron@ime.unicamp.br

† e-mail: clovis@ift.unesp.br

‡ e-mail: matsas@ift.unesp.br

- [1] J. Wisdom, *Science* **299**, 1865 (2003).
- [2] S. K. Blau, *Physics Today* **56**, 21 (2003); C. Seife, *Science* **299**, 1295 (2003).
- [3] A. Shapere and F. Wilczek, *Phys. Rev. Lett.* **58**, 2051 (1987); A. Shapere and F. Wilczek, *J. Fluid Mech.* **198**, 587 (1989); F. Wilczek and A. Shapere (Eds.), *Geometric Phases in Physics* (World Scientific, 1989).
- [4] S. Childress, *Mechanics of Swimming and Flying* (Cambridge University Press, Cambridge, 1978).
- [5] E. M. Purcell, *Am. J. Phys.* **45**, 3 (1977); E. M. Purcell, *Proc. Natl. Acad. Sci. U.S.A.* **94**, 11307 (1997); H. C. Berg, *Phys. Today* **53**, 24 (2000).
- [6] G. A. Landis, *Physics Today* **56**, 12 (2003); J. Wisdom, *Physics Today* **56**, 12 (2003).
- [7] M. J. Longo, *Am. J. Phys.* **72**, 1312 (2004).
- [8] G. A. Landis, *Acta Astronautica* **26**, 307 (1992); G. A. Landis and F. J. Hrach, *J. Guid. Control Dyn.* **14**, 214 (1991); M. Martinez-Sanchez and S. A. Gavit, *J. Guid. Control Dyn.* **10**, 233 (1987).
- [9] J. Walker, *Sci. Am.* **260**, 86 (March, 1989).
- [10] W. Rindler, *Am. J. Phys.* **34**, 1174 (1966).
- [11] A movie produced with two distinct numerical simulations emphasizing that the swinging and swimming effects tend to dominate in the low- and high-frequency regimes, respectively, is available in [http://www.ime.unicamp.br/~gueron/swim\\_vs\\_swing](http://www.ime.unicamp.br/~gueron/swim_vs_swing). For visualization purposes we have chosen  $GM = 1$ ,  $Gm_a = 0.1$ ,  $l = 1$ ,  $\Delta l = 1$ , and  $\alpha = 0.5$  with  $\Delta\alpha = 1$  and  $\alpha = 1.5$  with  $\Delta\alpha = -0.5$  in the first and second simulations, respectively.